Journal of Orthopaedic Translation 48 (2024) 190–203

Contents lists available at ScienceDirect

Journal of Orthopaedic Translation

journal homepage: www.journals.elsevier.com/journal-of-orthopaedic-translation

Original Article

METTL14-mediated HOXA5 m^{6}A modification alleviates osteoporosis via promoting WNK1 transcription to suppress NLRP3-dependent macrophage pyroptosis

Hao Tang [a,b], Yuxuan Du [a,b], Zejiu Tan [a,b], Dongpeng Li [a,b], Jiang Xie [a,b,*]

[a] Department of Spine Surgery and Orthopaedics, Xiangya Hospital, Central South University, Changsha, 410008, Hunan Province, China
[b] National Clinical Research Center for Geriatric Disorders, Xiangya Hospital, Central South University, Changsha, 410008, Hunan Province, China

ARTICLE INFO

Keywords:
HOXA5
METTL14
NLRP3
Osteoporosis
WNK1

ABSTRACT

Background: Osteoporosis is a commonly diagnosed metabolic bone disease. NLRP3 inflammasome activation and pyroptosis are observed during osteoporosis. However, the mechanism by which NLRP3-mediated pyroptosis contributes to osteoporosis remains largely undefined.

Methods: Ovariectomized (OVX) mice were employed as an *in vivo* model of osteoclastogenesis. H&E staining and micro-CT detected the histological changes and bone parameters in the femur tissues. RANKL-treated macrophages were used as the *in vitro* model of osteoclastogenesis, and LPS/ATP treatment was used as the macrophage pyroptosis model. The cytotoxicity, cytokine secretion and caspase-1 activity were assessed by LDH release assay, ELISA and flow cytometry, respectively. The osteoclast formation ability was detected by TRAP staining. qRT-PCR, IHC and Western blotting detected the expression and localization of METTL14, pyroptosis-related or osteoclast-specific molecules in femur tissues or macrophages. Mechanistically, MeRIP assessed the m^{6}A modification of *HOXA5*. Luciferase and ChIP assays were employed to detect the direct association between HOXA5 and *WNK1* promoter in macrophages.

Results: METTL14, HOXA5 and WNK1 were decreased in OVX mice, which was associated with pyroptosis. METTL14 or HOXA5 overexpression suppressed macrophage-osteoclast differentiation and pyroptosis, along with the upregulation of WNK1. METTL14-mediated m^{6}A modification stabilized *HOXA5* mRNA and increased its expression, and HOXA5 regulated *WNK1* expression via direct binding to its promoter. Functional studies showed that WNK1 knockdown counteracted METTL14- or HOXA5-suppressed pyroptosis and macrophage-osteoclast differentiation. In OVX mice, overexpression of METTL14 or HOXA5 alleviated osteoporosis via suppressing WNK1-dependent NLRP3 signaling.

Conclusion: METTL14-mediated *HOXA5* m^{6}A modification increased its expression, thereby inducing *WNK1* expression and suppressing NLRP3-dependent pyroptosis to alleviate osteoporosis. The combination of METTL14 or HOXA5 agonist with pyroptosis targeted therapy may be a promising therapeutic approach for osteoporosis.

The Translational Potential of this Article·:

- METTL14 or HOXA5 overexpression suppressed macrophage-osteoclast differentiation and pyroptosis in macrophages.·
- METTL14-mediated m6A modification stabilized HOXA5 mRNA and increased its expression.

Abbreviations: ATCC, American Type Culture Collection; BMD, bone mineral density; BMSCs, bone marrow mesenchymal stem cells; BV/TV, bone volume fraction; ChIP, chromatin immunoprecipitation; CTSK, cathepsin K; CTX-1, C-terminal telopeptide of Type-I collagen; GSDMD, gasdermin D; H&E, Hematoxylin & Eosin; HOXA5, homeobox protein A5; IDD, intervertebral disc degeneration; IGF2BP2, insulin-like growth factor 2 mRNA-binding proteins 2; IHC, immunohistochemistry; IL-1β, interleukin-1β; IL-18, interleukin-18; LDH, lactate dehydrogenase; LPS, lipopolysaccharide; m^{6}A, N^6-methyladenosine; MeRIP, methylated RNA immunoprecipitation; METTL14, methyltransferase-like 14; ncRNA, non-coding RNA; NFATc1, nuclear factor of activated T-cells cytoplasmic 1; NLRP3, nucleotide-binding oligomerization domain-like-receptor family pyrin domain-containing 3; NP, nucleus pulposus; OVX, ovariectomized; Tb.N, trabecular number; TBS, trabecular bone score; Tb.Th, trabecular thickness; TRAP, Tartrate Resistant Acid Phosphatase; WNK1, WNK lysine deficient protein kinase 1.

* Corresponding author. Department of Spine Surgery and Orthopaedic & National Clinical Research Center for Geriatric Disorders, Xiangya Road, Changsha, 410008, Hunan Province, China.

E-mail address: xj809902077@163.com (J. Xie).

https://doi.org/10.1016/j.jot.2024.08.008
Received 1 August 2023; Received in revised form 17 July 2024; Accepted 8 August 2024

- HOXA5 regulated WNK1 expression via direct binding to its promoter.
- Silencing of WNK1 reversed METTL14- or HOXA5-suppressed pyroptosis and macrophageosteoclast differentiation.·
- METTL14 or HOXA5 overexpression alleviated osteoporosis via suppressing WNK1-dependent NLRP3 signaling in OVX mice.

1. Introduction

Osteoporosis is one of the most frequently diagnosed metabolic bone disease which is characterized by impairment of bone mass, bone tissues and microarchitecture [1,2]. Patients with osteoporosis exhibited increased bone fragility and susceptibility to fracture [3]. The fracture incidence rates are raising as the population ages, leading to decreased life quality and economic burden worldwide [4]. Menopause and aging lead to imbalance between bone resorption and formation [2,3]. Except the universal recommendations for patients with osteoporosis, current osteoporosis therapies are classified into two groups: antiresorptive and anabolic agents [5]. Unraveling the molecular mechanism underlying imbalanced bone remodeling may provide novel insight for the choice of osteoporosis therapies.

The NLRP3 inflammasome is a large intracellular multiprotein complex which activated in response to pathogen- or damage-associated stimuli [6]. The NLRP3 inflammasome activates caspase-1, further leading to cleavage and production of IL-1β and IL-18, as well as GSDMD-mediated pyroptosis [6,7]. In recent years, emerging evidence supports the pivotal roles of NLRP3 inflammasome during osteoporosis [7]. Upon stimulation of aging or estrogen deficiency, NLRP3 inflammasome is activated, thus accelerating bone resorption and inhibiting bone formation via the release of IL-1β and IL-18 [7]. In ovariectomized (OVX) mice, NLRP3 inflammasome proteins are elevated in the femur, and lack of NLRP3 abrogates OVX-suppressed osteogenic differentiation [8]. Additionally, pyroptosis is commonly observed in osteoporosis [9]. However, the underlying mechanism by which NLRP3-mediated pyroptosis contributes to osteoporosis pathogenesis remains largely undefined. Interestingly, WNK lysine deficient protein kinase 1 (WNK1), a newly identified negative regulator of NLRP3, is downregulated in B cells derived from low bone mineral density (BMD) postmenopausal women [10,11], indicating its potential role in osteoporosis.

N^6-methyladenosine (m^6A) is the most abundant form of methylation in mRNA and non-coding RNA (ncRNA) [12]. Growing evidence has reported the critical role of m^6A in osteoporosis [13,14]. The m^6A 'writer', 'reader' and 'eraser' proteins play important roles in modifying RNA [12]. Recent studies have illustrated that methyltransferase-like 14 (METTL14), a m^6A 'writer' protein, is downregulated in bone specimens from patients with osteoporosis, and positively correlated with bone formation [15,16]. METTL14 overexpression promotes osteoblast proliferation, differentiation and mineral deposition [17]. Intriguingly, METTL14 inhibits NLRP3-mediated pyroptosis and diabetic cardiomyopathy through suppressing TINCR [18], raising the possibility that METTL14 might regulate bone remodeling via NLRP3-mediated pyroptosis in osteoporosis.

Homeobox protein A5 (HOXA5), a transcription factor, is implicated in the transcriptional regulation of bone-specific genes [19,20]. Previous studies have demonstrated that HOXA5 is markedly elevated in bone marrow mesenchymal stem cells (BMSCs) derived from aging mice, and overexpression of HOXA5 enhances osteoblast differentiation [21]. Bioinformatics analysis based on SRAMP database predicted the sites of m^6A modification in *HOXA5*, and JASPAR database predicted the putative binding sites of HOXA5 at *WNK1* promoter. We thus hypothesized that METTL14-mediated m^6A modification might stabilize *HOXA5* mRNA and increases its expression. The upregulated HOXA5 might induce WNK1 expression transcriptionally, thus suppressing NLRP3-mediated pyroptosis to alleviate osteoporosis.

In this study, we reported that METTL14 stabilized *HOXA5* mRNA by enhancing m^6A modification, thus increasing *WNK1* expression transcriptionally, ultimately suppressing NLRP3-dependent pyroptosis to alleviate osteoporosis. Our findings shed light on the crucial role of NLRP3-mediated pyroptosis in bone remodeling that could serve as a promising target for osteoporosis treatment.

2. Materials and methods

2.1. Animal study

All animal study was approved by Xiangya Hospital, Central South University. Female C57BL/6 (8-week-old, n = 6 per group) were purchased from SJA Laboratory Animal Co., Ltd (Hunan, China). OVX model was established as previously described [22]. Briefly, mice were anesthetized by isoflurane, and underwent bilateral ovariectomy via a midline abdominal incision. Mice in sham group received surgery without ovary removal. For *in vivo* overexpression study, the full-length of METTL14 or HOXA5 was cloned into HBAVV-CMV-T2A-GFP vector [23]. The overexpression construct pAAV-RC and pHelper were co-transfected into AAV-293 cells using LipoFiter reagent (Hanbio, Shanghai, China). For the METTL14 or HOXA5 overexpression, each mouse received 1×10^{11} V g AAV-METTL14 or AAV-HOXA5 via tail vein at 4 weeks post-surgery. Mice were sacrificed and the right femurs were dissected for subsequent analysis at 12 weeks after AAV injection.

2.2. Hematoxylin & Eosin (H&E) and immunohistochemistry (IHC)

The bone tissues were harvested and fixed in 4 % paraformaldehyde (PFA), decalcified in 10 % EDTA for 3 weeks, and embedded in paraffin. After deparaffinization and rehydration, the sections were stained with H&E reagent (Beyotime, Shanghai, China). For IHC analysis, the sections were subjected to antigen retrieval. After blocking, the slides were then stained with anti-NLRP3 (1:100, PA579740, Invitrogen, Carlsbad, CA, USA), anti-METTL14 (1:500, MA5-47189, Invitrogen), anti-HOXA5 (1:100, PA569008, Invitrogen) or anti-WNK1 (1:100, PA5-28382, Invitrogen) antibody at 4 °C overnight. This is followed by the incubation with secondary antibody-HRP, and the signal was detected using the DAB Development Kit (Beyotime).

2.3. Quantitative micro-CT

The right femurs were harvested and fixed in 4 % PFA, and scanned using a high-resolution micro-CT (Bruker microCT, Kontich, Belgium). Quantitative analysis of the bone parameters, including trabecular number (Tb.N), bone volume fraction (BV/TV) and trabecular thickness (Tb.Th) were performed.

2.4. ELISA assay

The whole blood was allowed to clot, and centrifuged at 1000×*g* for 10 min. The cell culture media were collected and centrifuged at 1500 rpm for 10 min. The serum or cell culture supernatant were subjected to ELISA assay. The serum or secreted levels of IL-1β and IL-18 were measured using commercial kits (88-7013-22 and KMC0181, Invitrogen) according to the manufacturer's protocols. The secretion and serum level of C-terminal telopeptide of Type-I collagen (CTX-1) was assessed using Mouse CTX-1 ELISA Kit (NBP3-11802, Novus, Centennial, CO, USA).

2.5. RNA isolation and qRT-PCR

Total RNA was isolated using Trizol reagent (Invitrogen) and reverse transcribed using PrimeScript RT Kit (TaKaRa, Dalian, China). qRT-PCR was conducted using SYBR Green Master Mix (Applied Biosystems, Foster City, CA, USA). The relative expression of target gene was calculated using $2^{-\Delta\Delta CT}$ method. For mRNA stability assay, macrophages were treated with 2 μg/mL Actinomycin D (Sigma–Aldrich, St Louis, MO, USA) for 0, 4, 8 and 12 h. The mRNA half-life of *HOXA5* was detected by qRT-PCR. Primers used in qRT-PCR was listed in Table 1.

2.6. Western blot analysis

Mouse tissues or cells were lysed using RIPA lysis buffer (Beyotime), and quantified using BCA Protein Assay Kit (Beyotime). Equal amounts of proteins were separated by gel electrophoresis and transferred onto PVDF membrane (Beyotime). After blocking with 5 % non-fat milk at room temperature for 1 h, the blots were probed with primary antibody at 4 °C overnight, followed by the incubation with secondary antibody-HRP. Signal was visualized using an ECL detection kit (Pierce, Rockford, IL, USA). Primary antibodies used in Western blotting: anti-METTL14 (1:1000, ab220030, Abcam), anti-HOXA5 (1:1000, MA5-19102, Invitrogen), anti-WNK1 (1:1000, PA5-28382, Invitrogen), anti-NLRP3 (1:1000, PA579740, Invitrogen), anti-Caspase-1 (1:1000, ab1384832, Abcam), anti-ASC (1:1000, ab309497, Abcam), anti-GSDMD (1:1000, ab209845, Abcam), anti-NFATc1 (1:1000, ab25916, Abcam), anti-CTSK (1:1000, ab19027, Abcam), anti-TRAP (1:1000, ab2391, Abcam) and anti-GAPDH (1:1000, ab8245, Abcam) antibodies.

2.7. Cell culture, treatment and transfection

RAW264.7 cells were purchased from ATCC (Manassas, VA, USA), and grown in DMEM containing 10 % FBS (Gibco, Grand Island, NY, USA). Bone marrow-derived macrophages (BMDMs) were isolated from femur and tibia of mice (8∼10-week old) as described [24]. BMDMs were grown in α-MEM supplemented with 10 % FBS and 30 mg/mL M-CSF (Gibco). All cells were maintained at 37 °C/5 % CO_2. For osteoclastogenesis, cells were treated with 10 ng/mL RANKL (Invitrogen) for 6 days [25]. For LPS/ATP stimulation, macrophages were primed with 200 ng/mL lipopolysaccharides (LPS, Sigma–Aldrich) for 6 h, and then incubated with 2 mM ATP (Sigma–Aldrich) for 30 min [26]. The full-length of METTL14 and HOXA5 were cloned into pcDNA3.1 vector (Invitrogen). ShMETTL14, shHOXA5, shWNK1 and shNC were purchased from GenePharma (Shanghai, China). RAW264.7 cells and BMDMs were transfection with overexpression plasmid and/or shRNA using Lipofectamine 3000 reagent (Invitrogen).

Table 1
Primers used for qRT-PCR analysis.

Genes	Primer sequences (5′-3′)
METTL14-F	GCTTGCGAAAGTGGGGTTAC
METTL14-R	AATGAAGTCCCCGTCTGTGC
HOXA5-F	CGCAAGCTGCACATTAGTCA
HOXA5-R	TTTCGATCCTTCTTCGGCGG
WNK1-F	TCCAACATCCTCAGCAGCAG
WNK1-R	GCTGACACTTGAGGCTGACT
IL-18-F	GGCTGCCATGTCAGAAGACT
IL-18-R	GGGTTCACTGGCACTTTGAT
IL-1β-F	GCCACCTTTTGACAGTGATGAG
IL-1β-R	AAGGTCCACGGGAAAGACAC
NFATc1-F	GGTGCTGTCTGGCCATAACT
NFATc1-R	GCGGAAAGGTGGTATCTCAA
CTSK-F	CTTCCAATACGTGCAGCAGA
CTSK-R	TTGCATCGATGGACACAGAG
TRAP-F	TGTTGACAGCGGTCCATCTA
TRAP-R	CCTCCTTCTTAACCCGAAGC
GAPDH-F	AGCCCAAGATGCCCTTCAGT
GAPDH-R	CCGTGTTCCTACCCCCAATG

2.8. LDH assay

LDH release was monitored using CyQUANT LDH Cytotoxicity Assay (Invitrogen). In brief, macrophages were cultured in 96-well plates overnight. The maximum LDH release was achieved by adding 10 × lysis buffer. The samples were incubated with 50 μL Reaction Mixture at room temperature for 30 min, followed by the incubation with Stop Solution. A490 and A680 were measured using a microplate reader (Thermo Fisher Scientific).

2.9. Flow cytometry

Caspase-1 activity was assessed using FAM-FLICA caspase-1 assay kit (Immunochemistry Technologies, Davis, CA, USA). Briefly, macrophages were stained with FLICA probe for 1 h, followed by staining with PI. Samples were analyzed by flow cytometry (BD Biosciences, San Jose, CA, USA).

2.10. TRAP assay

Cells were fixed with 4 % PFA and permeabilized with cold 50 %/50 % acetone/methanol. Osteoclasts were then stained with TRAP assay Kit (Beyotime). TRAP positive cells were visualized and counted under a microscopy (Nikon, Tokyo, Japan).

2.11. Methylated RNA immunoprecipitation (MeRIP)

mRNA was isolated using PolyATract mRNA Isolation System (Promega, Madison, WI, USA). MeRIP was performed using Magna MeRIP m^6A Kit (Millipore, Billerica, MA, USA). Briefly, mRNA was fragmented in Fragmentation Buffer at 94 °C for 4 min. The fragmented mRNA (5 μg) was then incubated with anti-m^6A antibody (5 μg)- or normal mouse IgG (5 μg)-conjugated Protein A/G beads at 4 °C for 2 h. The immunoprecipitated RNA was then eluted and purified, and the m^6A modification of *HOXA5* was analyzed by qRT-PCR.

2.12. Dual luciferase assay

The promoter region of *WNK1* was cloned into pGL-3 vector (Promega). RAW264.7 cells or BMDMs were co-transfected with shHOXA5, HOXA5 overexpression construct or corresponding control and luciferase construct using Lipofectamine 3000 (Invitrogen). The luciferase activity was measured using Dual-Luciferase Reporter Assay System (Promega) at 48 h post-transfection. Renilla activity was used as an internal control.

2.13. Chromatin immunoprecipitation (ChIP) assay

ChIP assay was performed using Pierce magnetic ChIP kit (Pierce). Briefly, macrophages were crosslinked using 1 % formaldehyde and lysed. After MNase digestion, the chromatin fractions were incubated with anti-HOXA5 (5 μg, sc-365784, Santa Cruz Biotechnologies, Santa Cruz, CA, USA), anti-H3 (2 μg, ab1791, Abcam) antibody or normal IgG at 4 °C overnight. Anti-H3 antibody and normal IgG acted as a positive and negative control, respectively. The purified DNA was subjected to qRT-PCR analysis.

2.14. Statistical analysis

All experiments were repeated for at least three time with triplicate assays. Data were analyzed using PRISM 8.0 (GraphPad, San Diego, CA, USA). Student's *t*-test or One-way ANOVA with Turkey post hoc test was conducted to assess the differences between two groups or multiple groups, respectively. $P < 0.05$ was considered statistically significant.

3. Results

3.1. METTL14, HOXA5 and WNK1 are downregulated in OVX mice with pyroptosis

To delineate the biological roles of METTL14, HOXA5 and WNK1 in OP, an OVX mouse model was established. As shown in Fig. 1A, H&E staining revealed remarkable bone loss in the femur of OVX mice, compared with that of sham mice. Both ELISA and qRT-PCR showed that IL-1β and IL-18 secretion and expression were dramatically increased in OVX group (Fig. 1B and C). Consistently, increased expression of NLRP3 was observed in the femur of OVX mice as detected by IHC analysis (Fig. 1D). By contrast, METTL14 was expressed in bone marrow cavity of sham mice, while the immunoreactivity of METTL14 in osteoblasts were markedly decreased in OVX mice (Fig. 1D). Additionally, the expression of HOXA5 and WNK1 in the femur were also assessed by IHC analysis. Similarly, HOXA5 and WNK1 were also expressed in bone marrow cavity of the femur, and their expression were downregulated in the femur of OVX mice (Fig. 1D). qRT-PCR further showed the reduction of *METTL14* and *HOXA5* in the femur of OVX mice (Fig. 1E and F). As presented in Fig. 1G, the protein levels of METTL14, HOXA5 and WNK1 were also decreased in the femur of OVX mice, accompanied with the induction of pyroptosis-related proteins NLRP3, caspase-1, ASC and GSDMD. Collectively, these findings suggest that METTL14, HOXA5 and WNK1 are downregulated in OVX mice, possibly associated with increased pyroptosis.

3.2. Overexpression of METTL14 or HOXA5 suppresses macrophage-osteoclast differentiation

To investigate the effects of METTL14 or HOXA5 on macrophage-osteoclast differentiation, overexpression experiments were conducted. As anticipated, transfection of *METTL14* or *HOXA5* overexpression construct successfully increased METTL14 or HOXA5 mRNA and protein levels in both RAW264.7 cells and BMDMs, respectively (Fig. 2A–D). TRAP assay showed that RANKL induced osteoclastogenesis in which the percentage of $TRAP^{+}$ cells were induced by RANKL, while METTL14 or HOXA5 overexpression attenuated this effect (Fig. 2E). As shown in Fig. 2F, the secretion of bone resorption marker CTX-1 was elevated upon RANKL treatment, whereas METTL14 or HOXA5 overexpression

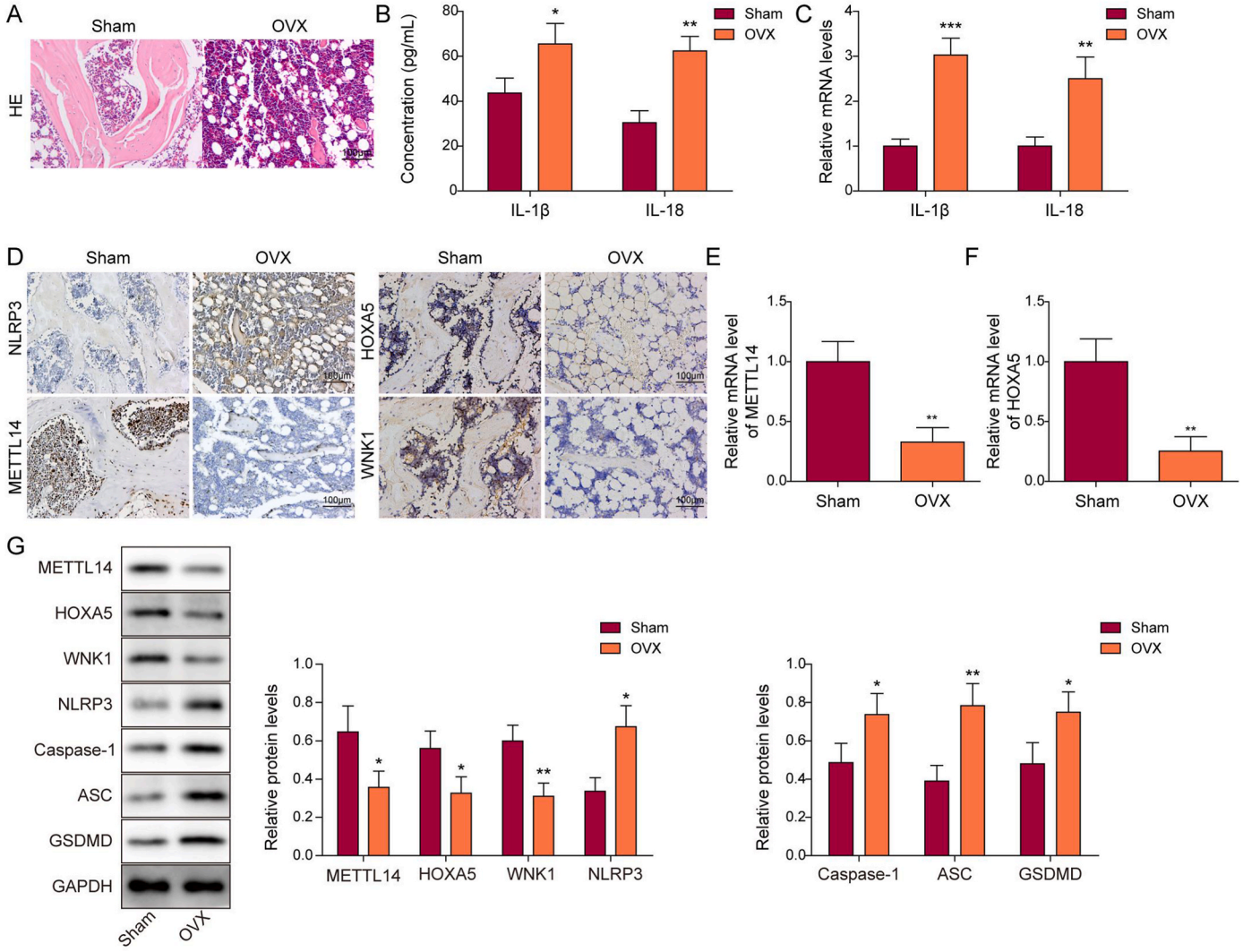

Figure 1. METTL14, HOXA5 and WNK1 are downregulated in OVX mice with pyroptosis. (A) The histological changes of femur were detected by H&E staining. Scale bar: 100 μm. n = 6 per group. (B) The serum levels of IL-1β and IL-18 were measured by ELISA assay. n = 6 per group. (C) The expression of *IL-1β* and *IL-18* in the femur were detected by qRT-PCR. n = 6 per group. (D) The immunoreactivities of NLRP3, METTL14, HOXA5 and WNK1 in the femur were examined by IHC analysis. Scale bar: 100 μm. n = 6 per group. (E&F) The mRNA levels of *METTL14* and *HOXA5* in the femur were detected by qRT-PCR. n = 6 per group. (G) The protein levels of METTL14, HOXA5, WNK1 and pyroptosis-related proteins in the femur were detected by Western blotting with quantitative analysis. n = 6 per group. *, $P < 0.05$; **, $P < 0.01$; ***, $P < 0.001$ as assessed by Student's *t*-test.

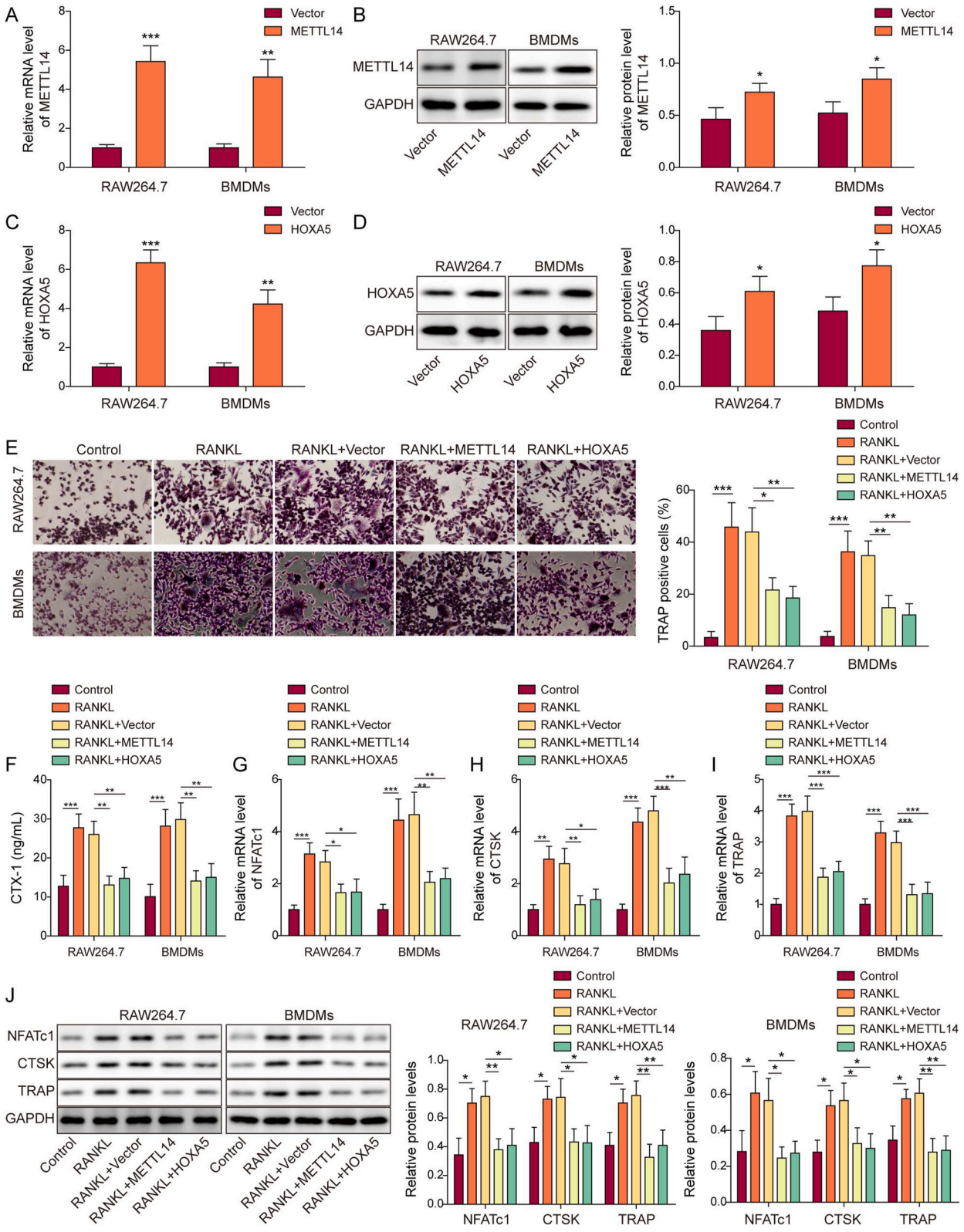

Figure 2. Overexpression of METTL14 or HOXA5 suppresses macrophage-osteoclast differentiation. (A, C) The mRNA levels of *METTL14* and HOXA5 in transfected macrophages were detected by qRT-PCR. n = 3. (B, D) The protein levels of METTL14 and HOXA5 in transfected macrophages were detected by Western blotting. n = 3. (E) RANKL-stimulated osteoclastogenesis in transfected macrophages was monitored by TRAP assay with quantitative analysis. The percentage of $TRAP^+$ multinucleated cells were counted and calculated. n = 3. (F) The secretion of CTX-1 was assessed by ELISA assay. n = 3. (G–I) The mRNA levels of osteoclast-specific molecules in transfected macrophages were detected by qRT-PCR. n = 3. (J) The protein levels of osteoclast-specific molecules in transfected macrophages were detected by Western blotting with quantitative analysis. n = 3. *, $P < 0.05$; **, $P < 0.01$; ***, $P < 0.001$ as assessed by Student's *t*-test (A–D) or One-way ANOVA with Turkey post hoc test (E–J).

abrogated RANKL-induced CTX-1 secretion. In line with these findings, osteoclast-specific molecules NFATc1, CTSK and TRAP were remarkably upregulated by RANKL, whereas METTL14 or HOXA5 overexpression abrogated RANKL-induced expression of these molecules in RAW264.7 cells and BMDMs as detected by qRT-PCR and Western blotting (Fig. 2G–J). These data indicate that METTL14 or HOXA5 overexpression impairs macrophage-osteoclast differentiation.

3.3. METTL14 or HOXA5 overexpression upregulates WNK1 expression and suppresses pyroptosis in macrophages

We further tested the functions of METTL14 and HOXA5 in the well-established LPS/ATP-induced pyroptosis model [27]. As presented in Fig. 3A, overexpression of METTL14 or HOXA5 rescued LPS/ATP-induced LDH release. qRT-PCR and ELISA assay unequivocally revealed that METTL14 or HOXA5 overexpression counteracted LPS/ATP-induced IL-1β and IL-18 secretion and expression in macrophages (Fig. 3B–E). Consistently, flow cytometry showed that LPS/ATP-increased caspase-1 activity was reversed by METTL14 or HOXA5 overexpression in which LPS/ATP-increased population of caspase-1^+/PI^+ cells were decreased in LPS+ATP + METTL14 or LPS + ATP + HOXA5 group (Fig. 3F). In accordance with these findings, Western blotting showed that METTL14 or HOXA5 overexpression abrogated LPS/ATP-downregulated WNK1, as well as LPS/ATP-upregulated pyroptosis-related proteins (Fig. 3G). These data suggest that METTL14 or HOXA5 upregulates WNK1 and inhibits pyroptosis in macrophages.

3.4. METTL14-mediated m^6A modification stabilizes HOXA5 mRNA and increases its expression

We next sought to test whether METTL14 was implicated in the m^6A modification of *HOXA5*. As expected, knockdown of METTL14 successfully downregulated METTL14 mRNA and protein levels in both RAW264.7 cells and BMDMs (Fig. 4A and B). In addition, qRT-PCR and Western blotting showed that METTL14 positively regulated HOXA5 expression in macrophages (Fig. 4C and D). MeRIP revealed that silencing of METTL14 decreased m^6A modification of *HOXA5*, while overexpression of METTL14 exerted an opposite effect (Fig. 4E). Furthermore, METTL14 knockdown impaired the mRNA stability of *HOXA5*, whereas METTL14 overexpression enhanced *HOXA5* mRNA stability (Fig. 4F). Taken together, these finding suggest that METTL14 plays an indispensable role in maintaining *HOXA5* mRNA stability via modulating m^6A modification.

3.5. HOXA5 regulates WNK1 expression via direct binding to its promoter

Bioinformatics analysis based on JASPAR database predicted the putative binding site of HOXA5 on *WNK1* promoter. To test whether HOXA5 regulated *WNK1* expression transcriptionally, gain- and loss-of function experiments were carried out. As presented in Fig. 5A and B, transfection of shHOXA5 markedly reduced HOXA5 mRNA and protein levels in both RAW264.7 cells and BMDMs. Consistently, silencing of HOXA5 downregulated WNK1 expression, while HOXA5 overexpression exerted an opposite effect on WNK1 expression (Fig. 5C and D). The potential binding site of HOXA5 was located at the promoter region of *WNK1* between nt −1639 and −1632 (Fig. 5E). The direction interaction between HOXA5 and *WNK1* promoter was further validated by ChIP assay in which antibody against HOXA5 successfully enriched *WNK1* promoter in both RAW264.7 cells and BMDMs (Fig. 5F). Dual luciferase reporter assay revealed that co-transfection of shHOXA5 and luciferase construct led to a dramatic reduction of luciferase activity, while increased luciferase activity was observed in HOXA5 overexpression group in macrophages (Fig. 5G). qRT-PCR and Western blotting further showed that METTL14-induced WNK1 expression was attenuated by shHOXA5 in macrophages (Fig. 5H and I). Collectively, these data indicate that METTL14 regulates WNK1 via modulating HOXA5, and HOXA5 regulates *WNK1* expression via direct binding to its promoter.

3.6. Knockdown of WNK1 reverses METTL14- or HOXA5-suppressed pyroptosis in macrophages

To explore the biological role of WNK1, knockdown studies coupled with functional experiments were carried out in macrophages. As expected, transfection of shWNK1 led to a reduction of WNK1 in both RAW264.7 cells and BMDMs (Fig. 6A and B). METTL14-suppressed LDH release was counteracted by shHOXA5 or shWNK1, and knockdown of WNK1 reversed HOXA5-inhibited LDH release (Fig. 6C). Similarly, qRT-PCR and ELISA assays revealed that knockdown of HOXA5 or WNK1 abrogated METTL14-decreased IL-1β and IL-18 secretion and expression, and WNK1 silencing counteracted HOXA5-decreased secretion and expression of IL-1β and IL-18 in macrophages (Fig. 6D–G). Flow cytometry further showed that HOXA5 or WNK1 knockdown rescued METTL14-impaired caspase-1 activity, and HOXA5-suppressed caspase-1 activity was reversed by shWNK1 (Fig. 6H). In line with these findings, METTL14 downregulated pyroptosis-related proteins, and silencing of HOXA5 or WNK1 resulted in a rebound of these proteins, and shWNK1 also attenuated HOXA5-mediated downregulation of pyroptosis-related proteins in RAW264.7 cells and BMDMs (Fig. 6I). Taken together, these data suggest that knockdown of WNK1 reverses METTL14- or HOXA5-suppressed pyroptosis in macrophages.

3.7. Silencing of WNK1 counteracts METTL14- or HOXA5-suppressed macrophage-osteoclast differentiation

We next investigated the function of WNK1 during macrophage-osteoclast differentiation. TRAP assay revealed that METTL14-suppressed osteoclastogenesis was reversed by shHOXA5 or shWNK1, and shWNK1 also abrogated HOXA5-suppressed macrophage-osteoclast differentiation (Fig. 7A). In consistent with this finding, METTL14-decreased osteoclast-specific molecules were rescued by shHOXA5 or shWNK1, and HOXA5-reduced these proteins were also reversed by shWNK1 as detected by qRT-PCR and Western blotting (Fig. 7B–E). We further investigated the effects of WNK1 and NLRP3 on osteoclast formation. As shown in Figs. S1A–D, overexpression of WNK1 or NLRP3 successfully upregulated WNK1 or NLRP3 mRNA and protein levels in RAW264.7 cells and BMDMs. Moreover, the percentage of $TRAP^+$ cells were decreased in WNK1-ovexpressing macrophages upon RANKL treatment, while co-transfection of WNK1 and NLRP3 led to a rebound of $TRAP^+$ cell proportion in macrophages (Fig. S1E). Consistently, WNK1 overexpression reduced osteoclast-specific molecules NFATc1, CTSK and TRAP in RANKL-treated macrophages, while overexpression of NLRP3 further compensated for the loss of these proteins (Figs. S1F–I). Together, these findings indicate that WNK1 functions as an important downstream effector in METTL14- or HOXA5-suppressed macrophage-osteoclast differentiation.

3.8. Overexpression of METTL14 or HOXA5 alleviates osteoporosis via suppressing WNK1-dependent NLRP3 signaling in vivo

The *in vitro* findings were further validated in OVX mice. As shown in Fig. 8A–H&E staining revealed that overexpression of METTL14 or HOXA5 rescued OVX-induced bone loss. Compared with sham mice, the bone parameters, including bone volume fraction (BV/TV), trabecular number (Tb.N) and trabecular thickness (Tb.Th), were remarkable decreased in OVX mice (Fig. 8B–D). METTL14 or HOXA5 overexpression caused a rebound of these bone parameters (Fig. 8B–D). Consistent with the *in vitro* findings, the serum level of CTX-1 was increased in OVX mice, while it was attenuated in OVX + METTL14 or OVX + HOXA5 mice (Fig. 8E). We next tested the effects of METTL14 or HOXA5 on NLRP3-dependent pyroptosis. As anticipated, the secretion and expression of IL-1β and IL-18 were greatly elevated in OVX mice, whereas

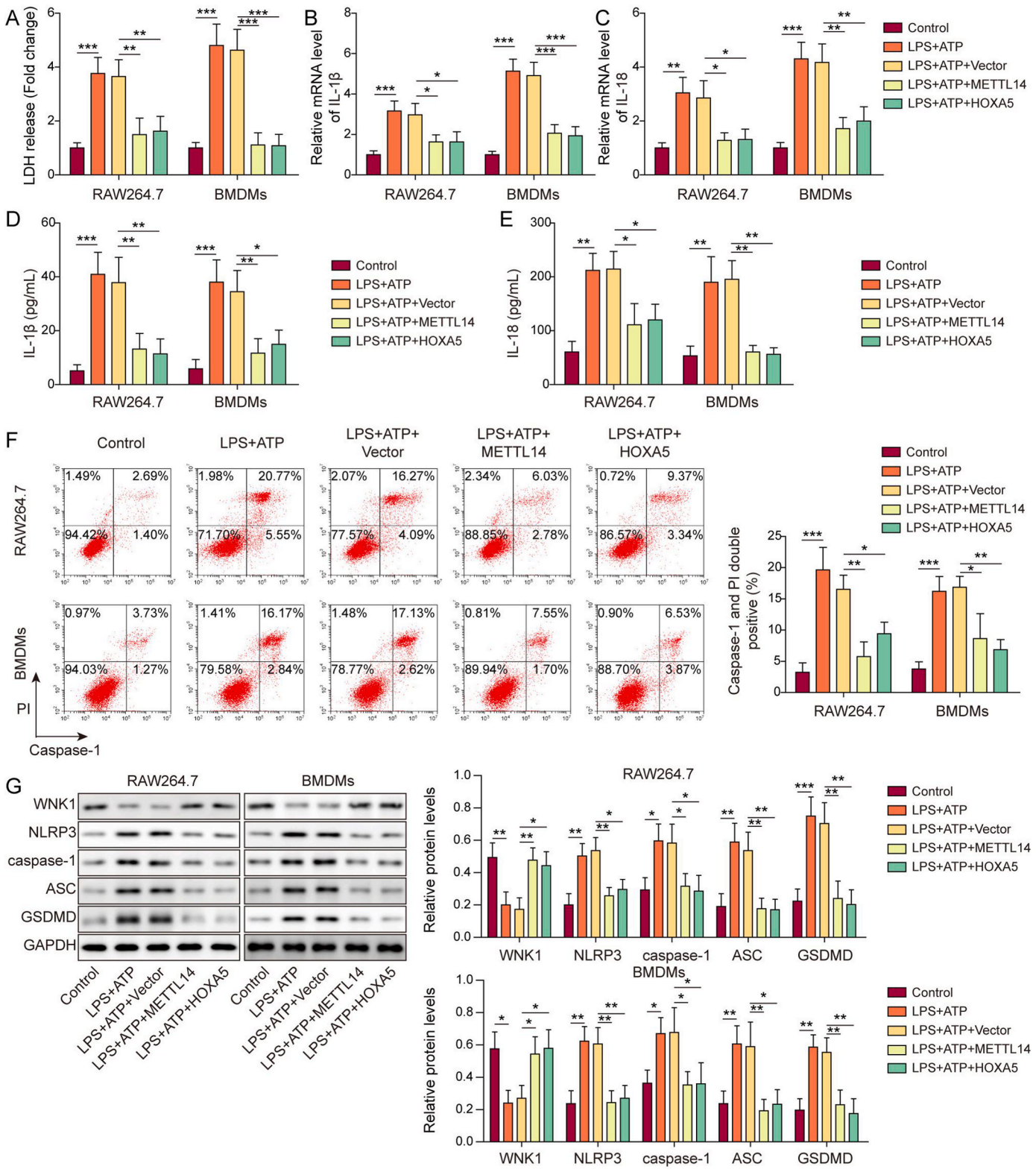

Figure 3. METTL14 or HOXA5 overexpression upregulates WNK1 expression and suppresses pyroptosis in macrophages. (A) LDH release in transfected macrophages was monitored using commercial kit. n = 3. (B&C) The mRNA levels of *IL-1β* and *IL-18* in transfected macrophages were detected by qRT-PCR. n = 3. (D&E) The secreted IL-1β and IL-18 levels in the cell culture supernatant were measured by ELISA assay. n = 3. (F) The populations of caspase-1^{+}/PI^{+} cells were analyzed by flow cytometry with quantitative analysis. n = 3. (G) The protein levels of WNK1 and pyroptosis-related proteins in transfected macrophages were detected by Western blotting with quantitative analysis. n = 3. *, P < 0.05; **, P < 0.01; ***, P < 0.001 as assessed by One-way ANOVA with Turkey post hoc test.

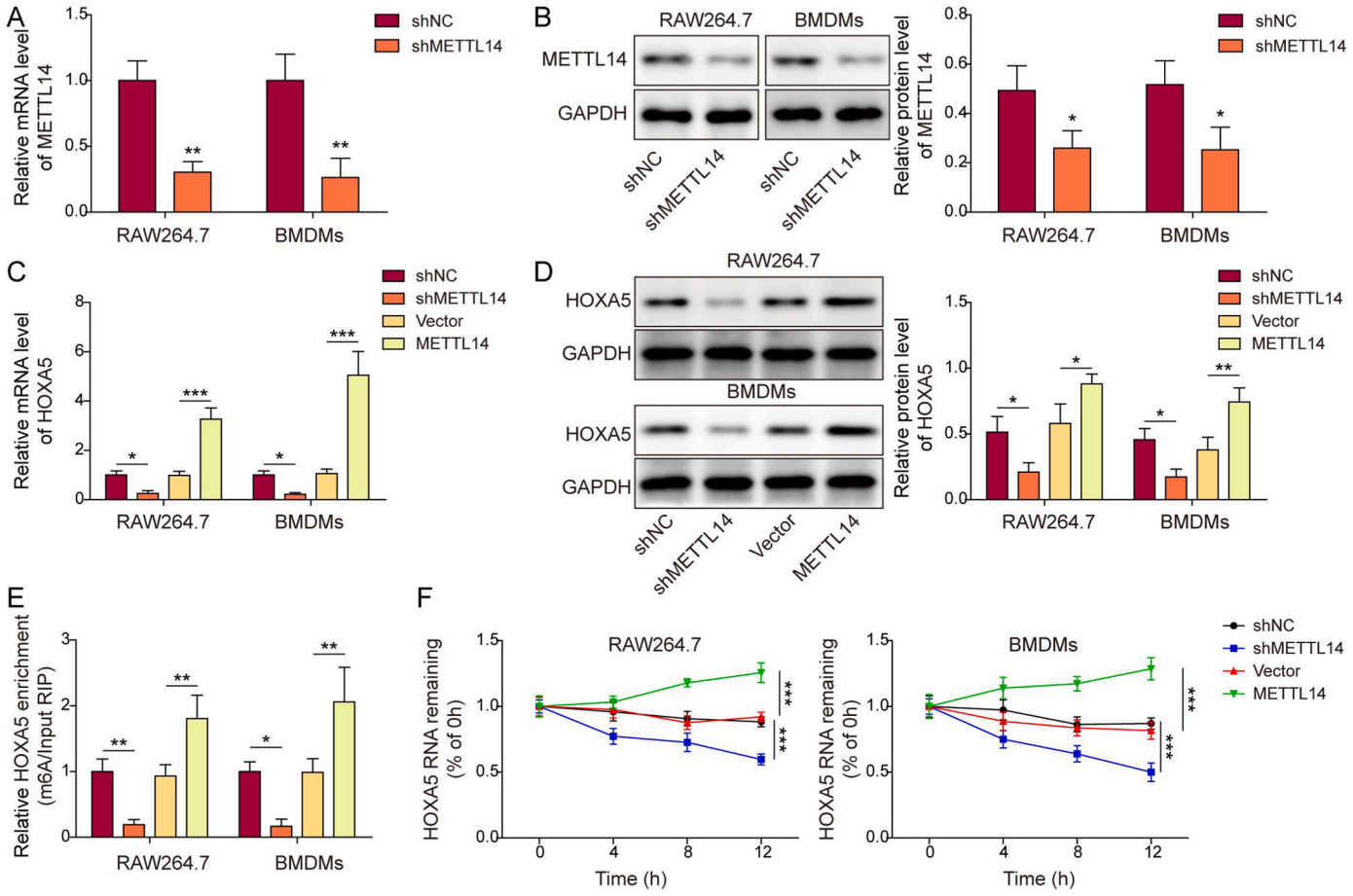

Figure 4. METTL14-mediated m^{6}A modification stabilizes HOXA5 mRNA and increases its expression. (A, C) The mRNA level of METTL14 or HOXA5 in transfected macrophages was detected by qRT-PCR. n = 3. (B, D) The protein level of METTL14 or HOXA5 in transfected macrophages was detected by Western blotting with quantitative analysis. n = 3. (E) The m^{6}A modification of HOXA5 in transfected macrophages was evaluated by MeRIP. n = 3. (F) HOXA5 mRNA stability in transfected macrophages was assessed by RNA stability assay. n = 3. *, P < 0.05; **, P < 0.01; ***, P < 0.001 as assessed by Student's *t*-test.

METTL14 or HOXA5 overexpression attenuated these effects as detected by ELISA assay and qRT-PCR, respectively (Fig. 8F–I). IHC analysis further showed that OVX-induced NLRP3 in the femur was abolished by METTL14 or HOXA5 overexpression (Fig. 8J). The successful overexpression of METTL14 or HOXA5 was confirmed by Western blotting (Fig. 8K). In addition, METTL14 or HOXA5 overexpression also resulted in an elevation of WNK1 in the femur of OVX mice, along with the downregulation of pyroptosis-related proteins (Fig. 8K). As shown in Fig. 8L, injection of AAV-METTL14 or AAV-HOXA5 also successfully upregulated METTL14 or HOXA5 expression in BMDMs isolated from mouse bone marrow. These data suggest that METTL14 or HOXA5 ameliorates osteoporosis via regulating WNK1, thereby suppressing NLRP3-dependent pyroptosis.

4. Discussion

Osteoporosis frequently occurs in postmenopausal women and elderly people [1]. Osteoporosis-related fractures resulted in lower overall physical function, as well as increased economic burden for healthcare system [2,3]. Understanding the mechanism underlying osteoporosis pathogenesis will provide further insight into targeted therapy for osteoporosis. In this study, we demonstrated that METTL14 stabilizes *HOXA5* mRNA and increases its expression by enhancing m^{6}A modification. The upregulated HOXA5 further increases WNK1 expression via direct binding to its promoter, thereby suppressing NLRP3-dependent pyroptosis to alleviate osteoporosis. Current therapies targeting pyroptosis are effective in bone metabolic diseases, including osteoporosis [7,28]. Our findings suggest that the combination of METTL14 or HOXA5 agonist with pyroptosis targeted therapy may be a promising therapeutic approach for osteoporosis.

Accumulating evidence illustrates that m^{6}A modification is implicated in the regulation of various biological or pathological processes, such as differentiation of BMSCs, osteoblasts or osteoclasts, as well as bone resorption [29]. METTL14, a core member of m^{6}A methyltransferase complex, is implicated in the methylation of mRNA and ncRNA [14]. Despite *METTL14* shares 43 % sequence identity with *METTL3*, METTL14 alone exhibits undetectable catalytic activity [30,31]. Accumulating evidence supports the role of METTL14-mediated m^{6}A modification in bone diseases. For instance, METTL14 enhances osteogenic differentiation of BMSCs through triggering autophagy via m^{6}A/IGF2BPs/Beclin-1 axis [32]. In addition, a recent study has illustrated that exosomal METTL14 regulates osteoclast bone absorption via modulating m^{6}A modification of *NFATc1* [33]. Interestingly, METTL14 is a direct target of miR-103-3p in MC3T3-E1 preosteoclasts, and METTL14-mediated m^{6}A modification modulates miR-103-3p processing by binding to DGCR8, thereby promoting osteoblastic bone formation [17]. In accordance with these findings, we found that METTL14 was decreased in OVX mice, and it suppressed macrophage-osteoclast differentiation and pyroptosis in macrophages. Mechanistically, METTL14-dependent m^{6}A mRNA methylation plays an indispensable role in maintaining *HOXA5* mRNA stability. It is worth noting that METTL14 mediates m^{6}A modification of *NLRP3* and stabilizes its mRNA in an IGF2BP2-dependent manner in nucleus pulposus (NP) cells [34]. Whether METTL14 modulates *NLRP3* mRNA stability in macrophages

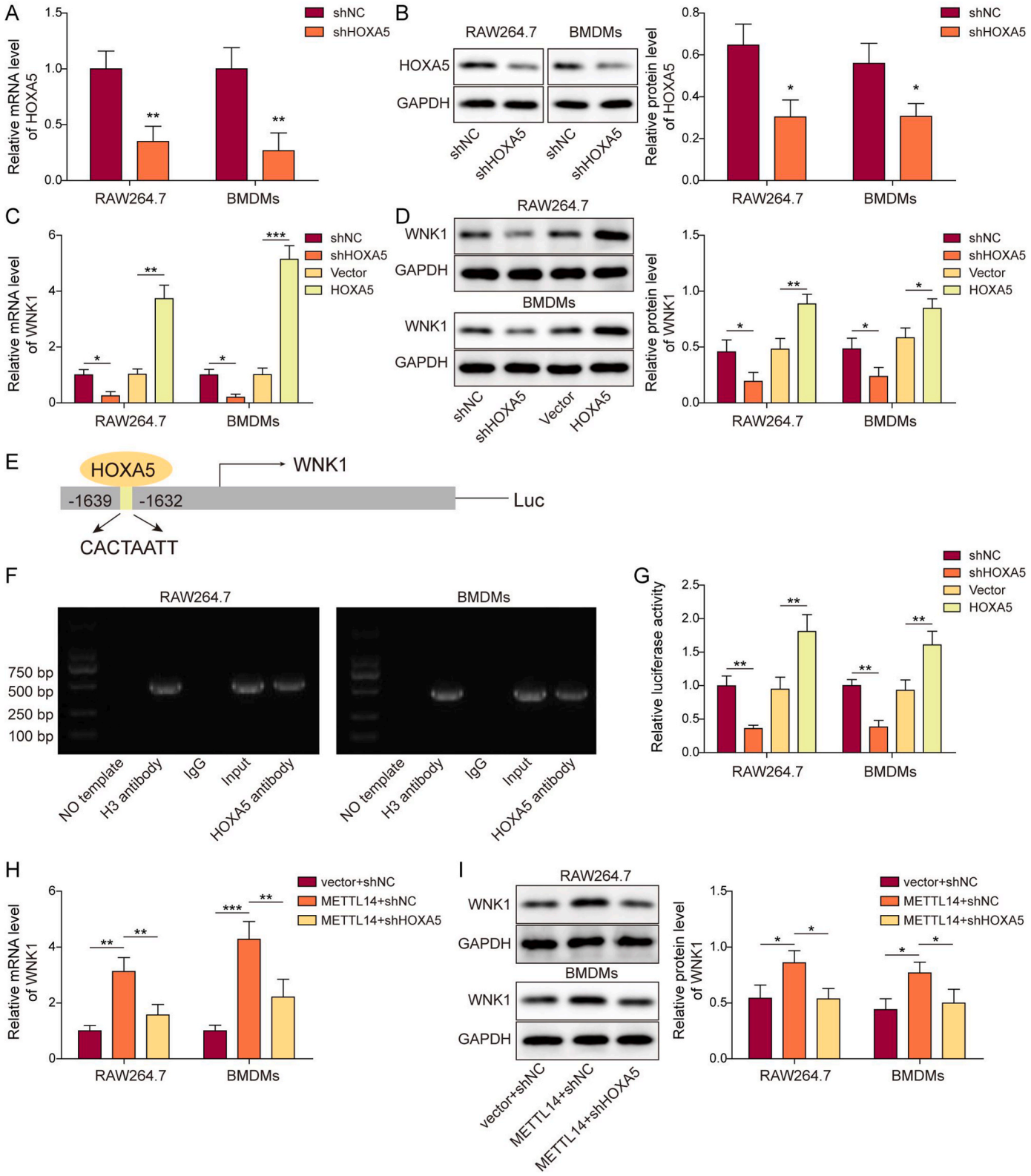

Figure 5. HOXA5 regulates WNK1 expression via direct binding to its promoter. (A, C) The mRNA level of *HOXA5* or *WNK1* in transfected macrophages was detected by qRT-PCR. n = 3. (B, D) The protein level of HOXA5 or WNK1 in transfected macrophages was detected by Western blotting with quantitative analysis. n = 3. (E) The putative binding site between HOXA5 and WNK1 promoter. n = 3. (F) The direct interaction between HOXA5 and *WNK1* promoter in macrophages was detected by ChIP assay. n = 3. PCR products were assessed by agarose gel electrophoresis. Anti-H3 antibody and normal IgG served as a positive and negative control, respectively. n = 3. (G) The relative luciferase activity in transfected macrophages was assessed by dual luciferase assay. n = 3. (H&I) The mRNA and protein levels of WNK1 in transfected macrophages were detected by qRT-PCR and Western blotting with quantitative analysis, respectively. n = 3. *, $P < 0.05$; **, $P < 0.01$; ***, $P < 0.001$ as assessed by Student's *t*-test (A&B) or One-way ANOVA with Turkey post hoc test (C–I).

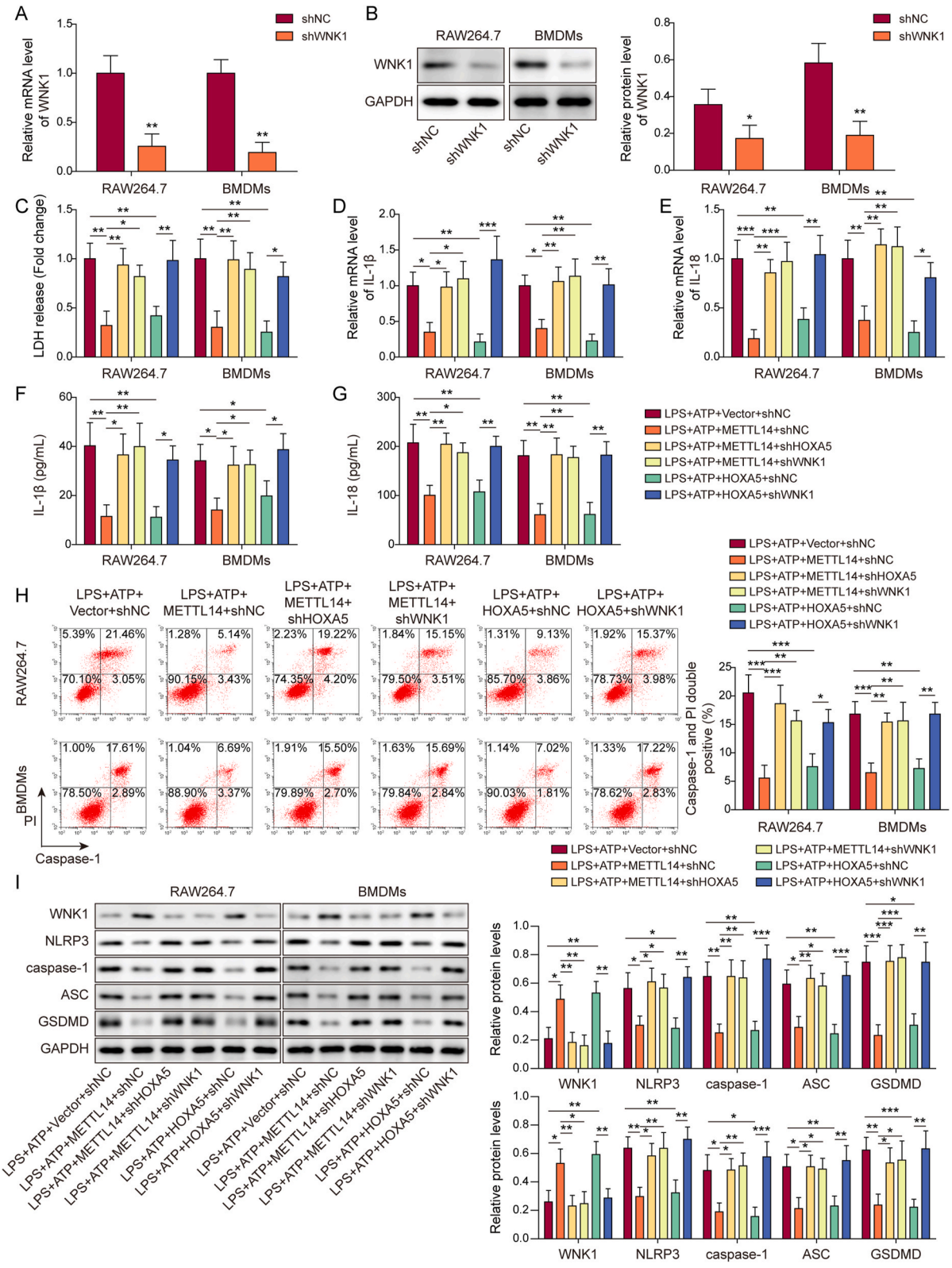

Figure 6. Knockdown of WNK1 reverses METTL14- or HOXA5-suppressed pyroptosis in macrophages. (A) The mRNA level of WNK1 in transfected macrophages was detected by qRT-PCR. n = 3. (B) The protein level of WNK1 in transfected macrophages was detected by Western blotting with quantitative analysis. n = 3. (C) LDH release in transfected macrophages was monitored using commercial kit. n = 3. (D&E) The mRNA levels of *IL-1β* and *IL-18* in transfected macrophages were detected by qRT-PCR. n = 3. (F&G) The secreted IL-1β and IL-18 levels in the cell culture supernatant were measured by ELISA assay. n = 3. (H) The populations of caspase-1^{+}/PI^{+} cells were analyzed by flow cytometry with quantitative analysis. n = 3. (I) The protein levels of WNK1 and pyroptosis-related proteins in transfected macrophages were detected by Western blotting with quantitative analysis. n = 3. *, $P < 0.05$; **, $P < 0.01$; ***, $P < 0.001$ as assessed by Student's *t*-test (A&B) or One-way ANOVA with Turkey post hoc test (C–I).

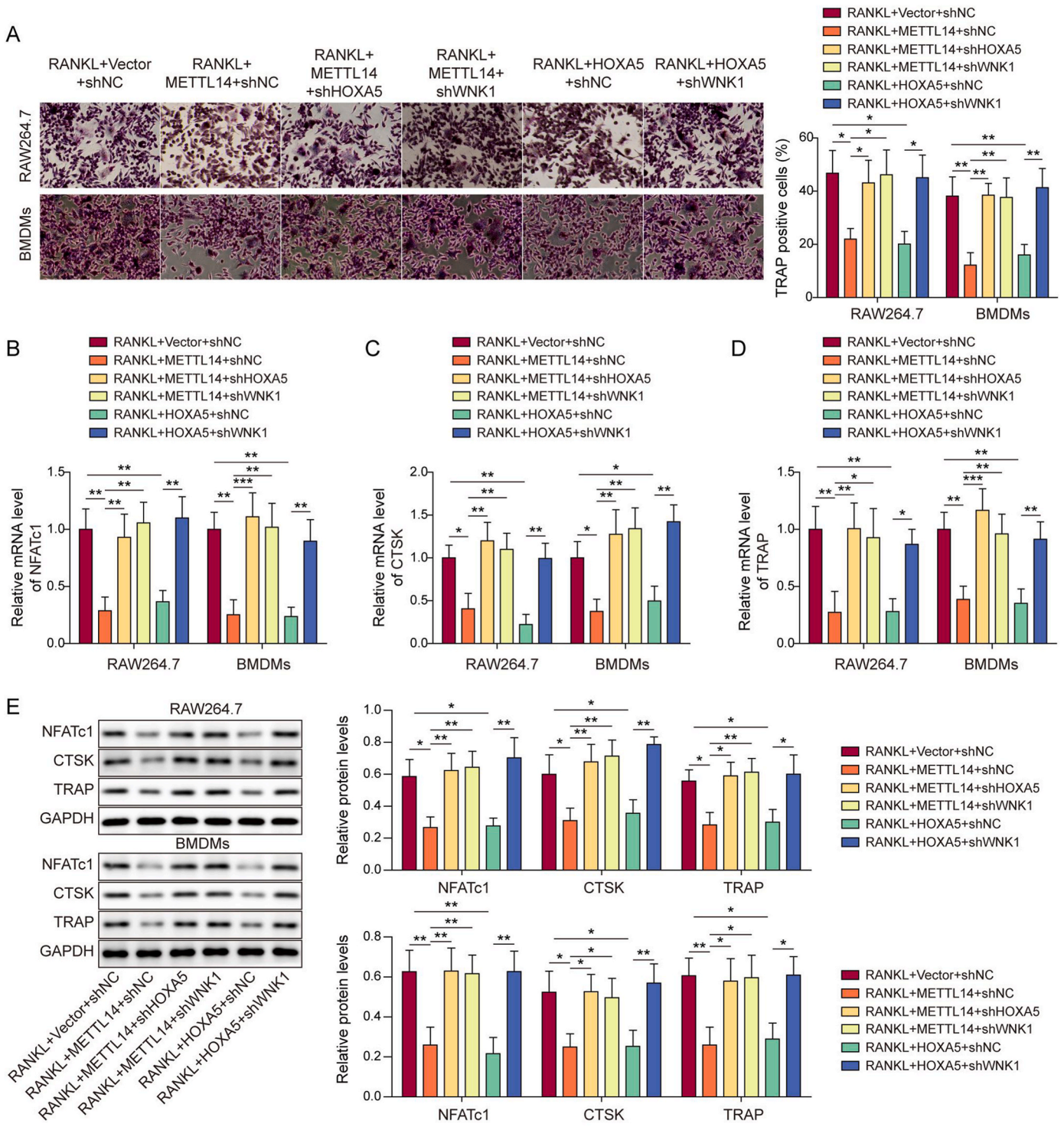

Figure 7. Silencing of WNK1 counteracts METTL14- or HOXA5-suppressed macrophage-osteoclast differentiation. (A) RANKL-stimulated osteoclastogenesis in transfected macrophages was monitored by TRAP assay with quantitative analysis. The percentage of $TRAP^{+}$ multinucleated cells were counted and calculated. n = 3. (B–D) The mRNA levels of osteoclast-specific molecules in transfected macrophages were detected by qRT-PCR. n = 3. (E) The protein levels of osteoclast-specific molecules in transfected macrophages were detected by Western blotting with quantitative analysis. n = 3. *, $P < 0.05$; **, $P < 0.01$; ***, $P < 0.001$ as assessed by One-way ANOVA with Turkey post hoc test.

merits further investigation in the future study. Our findings illustrated that METTL14 suppressed macrophage-osteoclast differentiation. However, the role of METTL14 in osteoblastic differentiation remains uninvestigated.

HOXA5 belongs to HOX family which plays diverse roles in skeletal development and fracture healing [35,36]. A recent study has illustrated that miR-19a-3p modulates osteogenic differentiation through targeting HOXA5 in BMSCs [21]. In addition, miR-23a cluster decreases the recruitment of HOXA5 and HOXA11 to bone-specific promoters and suppresses histone H3 acetylation during osteogenic differentiation [20]. In adipocytes, mechanistic study has showed that HOXA5 suppresses inflammation, accompanied with the downregulation of NLRP3

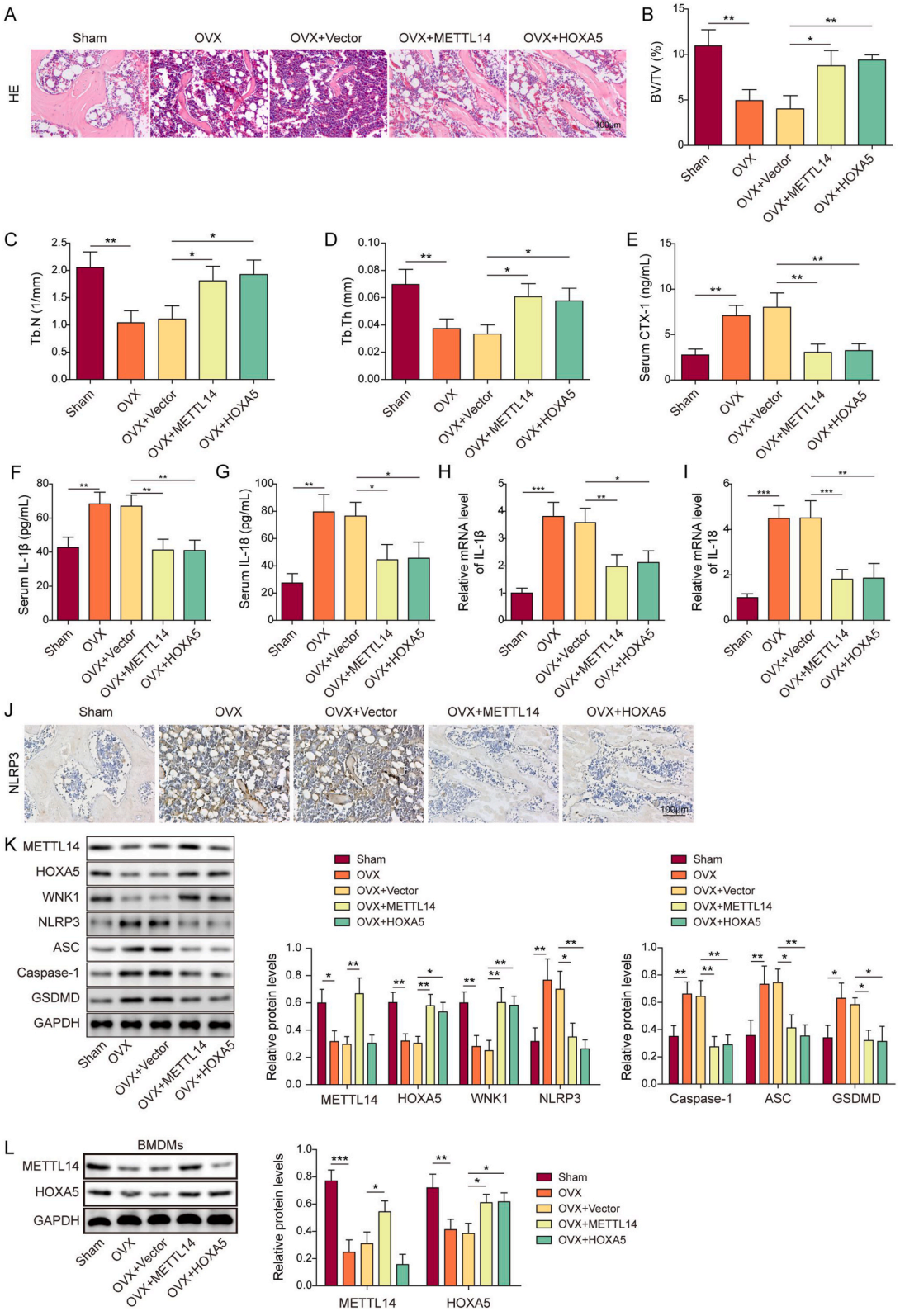

Figure 8. Overexpression of METTL14 or HOXA5 alleviates osteoporosis via suppressing WNK1-dependent NLRP3 signaling *in vivo*. (A) The histological changes of femur were detected by H&E staining. Scale bar: 100 μm. n = 6 per group. (B–D) BV/TV, Tb.N and Tb.Th were measured by micro-CT. n = 6 per group. (E) The serum level of CTX-1 was assessed by ELISA assay. n = 6 per group. (F&G) The serum levels of IL-1β and IL-18 were measured by ELISA assay. n = 6 per group. (H&I) The expression of *IL-1β* and *IL-18* in the femur were detected by qRT-PCR. n = 6 per group. (J) The immunoreactivity of NLRP3 in the femur was examined by IHC analysis. Scale bar: 100 μm. n = 6 per group. (K) The protein levels of METTL14, HOXA5, WNK1 and pyroptosis-related proteins in the femur were detected by Western blotting with quantitative analysis. n = 6 per group. (L) The protein levels of METTL14 and HOXA5 in BMDMs were detected by Western blotting with quantitative analysis. n = 6 per group. *, P < 0.05; **, P < 0.01; ***, P < 0.001 as assessed by One-way ANOVA with Turkey post hoc test.

[37]. However, little is known about the post-transcriptional modification of *HOXA5*, especially METTL14-mediated m^{6}A modification. In this study, we demonstrated that HOXA5 inhibited macrophage-osteoclast differentiation and NLRP3-dependent pyroptosis. Besides METTL14-mediated *HOXA5* m^{6}A modification, our findings also delineated the downstream signaling of HOXA5 in osteoporosis.

The mechanism by which HOXA5 reduces NLRP3 remains elusive. In the current study, WNK1, a transcriptional target of HOXA5, was identified as an important mediator in this regulatory axis. HOXA5 upregulated WNK1 expression via binding to its promoter. Interestingly, lacking WNK1 induces NLRP3 activation and pyroptosis in macrophages [11]. Consistent with this report, our data illustrated that silencing of WNK1 counteracted METTL14- or HOXA5-suppressed NLRP3-dependent pyroptosis *in vitro*. In OVX mice, METTL14 or HOXA5 overexpression resulted in the downregulation of NLRP3 signaling proteins, along with the upregulation of WNK1. Further *in vivo* rescue experiments are required to validate if WNK1 serves as a mediator in METTL14/HOXA5-regulated pyroptosis in the future study. Moreover, it is worth noting that WNK1 was decreased in the femur of OVX mice, and this is consistent with the previous report which demonstrated the reduced expression of WNK1 in B cells derived from low BMD postmenopausal women [10]. Our findings first demonstrated that WNK1 acted as a critical downstream effector of METTL14/HOXA5 during osteogenic differentiation.

NLRP3 inflammasome activates caspase-1 to process precursors IL-1β and IL-18, leading to the release of mature IL-1β and IL-18 [7]. On one hand, IL-1β acts as an osteogenic inhibitor by suppressing BMP/Smad signaling and osteogenic markers [38]. On the other hand, IL-1β induces RANKL to facilitate osteoclast differentiation and activation [39,40]. The role of IL-18 in osteoclastogenesis remains controversial [41]. It was identified as an osteoclastogenic cytokine [42], while another study has reported the synergistic action of IL-12 and IL-18 on suppressing osteoclast formation [43]. In this study, the elevation of IL-1β and IL-18 were found in OVX mice and LPS/ATP-stimulated macrophages, accompanied with the activation of caspase-1. In addition to the inflammatory responses through IL-1β and IL-18, NLRP3 inflammasome also induces pyroptosis in osteoporosis [7,9]. The induction of IL-1β and IL-18 cause death of osteoblast, and ROS, which is derived from NLRP3 activation, induces pyroptosis of osteoblast *in vitro* [9,44]. Recent studies have demonstrated the regulatory mechanism underlying pyroptosis in bone diseases [45,46]. For instance, LKB1/AMPK signaling suppresses NLRP3 inflammasome-dependent pyroptosis in osteoarthritis [46]. In addition, human adipose tissue stem cells-derived exosomal miR-155-5p ameliorates intervertebral disc degeneration (IDD) through targeting TGFβR2 to facilitate autophagy and inhibit pyroptosis [45]. We showed that OVX- or LPS/ATP-induced pyroptosis was attenuated by METTL14 or HOXA5, and WNK1 functioned as a downstream effector during this process. Our findings broaden the understanding of NLRP3-induced pyroptosis in osteoporosis, and provide novel insight into the pyroptosis targeted therapy for osteoporosis.

In conclusion, we demonstrated that METTL14-stabilized *HOXA5* inhibited NLRP3-dependent pyroptosis via modulating WNK1 expression transcriptionally, thereby alleviating osteoporosis. These findings indicate that pharmacological regulation of this regulatory axis, in particular METTL14 or HOXA5 agonist, may improve the clinical outcomes of osteoporosis.

Ethics approval and consent to participate

All animal study was approved by the Ethics Committee of Xiangya Hospital, Central South University, approval number [202103372].

Consent for publication

Not applicable.

Availability of data and materials

The datasets generated during and/or analysed during the current study are available from the corresponding author on reasonable request.

Funding

This study was supported by the Fundamental Research Funds for the Central Universities of Central South University.

CRediT authorship contribution statement

Hao Tang: Conceptualization, Writing – original draft, Methodology, Validation, Project administration. **Yuxuan Du:** Resources, Data curation. **Zejiu Tan:** Formal analysis, Investigation. **Dongpeng Li:** Visualization. **Jiang Xie:** Supervision, Writing – review & editing, Funding acquisition.

Declaration of competing interest

The authors declare that they have no known competing financial interests or personal relationships that could have appeared to influence the work reported in this paper.

Appendix A. Supplementary data

Supplementary data to this article can be found online at https://doi.org/10.1016/j.jot.2024.08.008.

References

[1] Rachner TD, Khosla S, Hofbauer LC. Osteoporosis: now and the future. Lancet 2011;377(9773):1276–87.
[2] Sozen T, Ozisik L, Basaran NC. An overview and management of osteoporosis. Eur J Rheumatol 2017;4(1):46–56.
[3] Akkawi I, Zmerly H. Osteoporosis: current concepts. Joints 2018;6(2):122–7.
[4] Clynes MA, Harvey NC, Curtis EM, Fuggle NR, Dennison EM, Cooper C. The epidemiology of osteoporosis. Br Med Bull 2020;133(1):105–17.
[5] Minisola S, Cipriani C, Occhiuto M, Pepe J. New anabolic therapies for osteoporosis. Intern Emerg Med 2017;12(7):915–21.
[6] Swanson KV, Deng M, Ting JP. The NLRP3 inflammasome: molecular activation and regulation to therapeutics. Nat Rev Immunol 2019;19(8):477–89.
[7] Jiang N, An J, Yang K, Liu J, Guan C, Ma C, et al. NLRP3 inflammasome: a new target for prevention and control of osteoporosis? Front Endocrinol 2021;12:752546.
[8] Xu L, Zhang L, Wang Z, Li C, Li S, Li L, et al. Melatonin suppresses estrogen deficiency-induced osteoporosis and promotes osteoblastogenesis by inactivating the NLRP3 inflammasome. Calcif Tissue Int 2018;103(4):400–10.
[9] Tao Z, Wang J, Wen K, Yao R, Da W, Zhou S, et al. Pyroptosis in osteoblasts: a novel hypothesis underlying the pathogenesis of osteoporosis. Front Endocrinol 2020;11:548812.
[10] Xiao P, Chen Y, Jiang H, Liu YZ, Pan F, Yang TL, et al. In vivo genome-wide expression study on human circulating B cells suggests a novel ESR1 and MAPK3 network for postmenopausal osteoporosis. J Bone Miner Res 2008;23(5):644–54.
[11] Mayes-Hopfinger L, Enache A, Xie J, Huang CL, Kochl R, Tybulewicz VLJ, et al. Chloride sensing by WNK1 regulates NLRP3 inflammasome activation and pyroptosis. Nat Commun 2021;12(1):4546.
[12] Coker H, Wei G, Brockdorff N. m6A modification of non-coding RNA and the control of mammalian gene expression. Biochim Biophys Acta Gene Regul Mech 2019;1862(3):310–8.
[13] Chen X, Hua W, Huang X, Chen Y, Zhang J, Li G. Regulatory role of RNA N(6)-methyladenosine modification in bone biology and osteoporosis. Front Endocrinol 2019;10:911.
[14] Hu Y, Zhao X. Role of m6A in osteoporosis, arthritis and osteosarcoma. Exp Ther Med 2021;22(3):926.
[15] Deng M, Luo J, Cao H, Li Y, Chen L, Liu G. METTL14 represses osteoclast formation to ameliorate osteoporosis via enhancing GPX4 mRNA stability. Environ Toxicol 2023;38(9):2057–68.
[16] Wang C, Chen R, Zhu X, Zhang X, Lian N. METTL14 alleviates the development of osteoporosis in ovariectomized mice by upregulating m(6)A level of SIRT1 mRNA. Bone 2023;168:116652.
[17] Sun Z, Wang H, Wang Y, Yuan G, Yu X, Jiang H, et al. MiR-103-3p targets the m(6)A methyltransferase METTL14 to inhibit osteoblastic bone formation. Aging Cell 2021;20(2):e13298.

[18] Meng L, Lin H, Huang X, Weng J, Peng F, Wu S. METTL14 suppresses pyroptosis and diabetic cardiomyopathy by downregulating TINCR lncRNA. Cell Death Dis 2022;13(1):38.
[19] Chen H, Rubin E, Zhang H, Chung S, Jie CC, Garrett E, et al. Identification of transcriptional targets of HOXA5. J Biol Chem 2005;280(19):19373–80.
[20] Godfrey TC, Wildman BJ, Beloti MM, Kemper AG, Ferraz EP, Roy B, et al. The microRNA-23a cluster regulates the developmental HoxA cluster function during osteoblast differentiation. J Biol Chem 2018;293(45):17646–60.
[21] Chen S, Li Y, Zhi S, Ding Z, Huang Y, Wang W, et al. lncRNA xist regulates osteoblast differentiation by sponging miR-19a-3p in aging-induced osteoporosis. Aging Dis 2020;11(5):1058–68.
[22] Thompson DD, Simmons HA, Pirie CM, Ke HZ. FDA Guidelines and animal models for osteoporosis. Bone 1995;17(4 Suppl). 125S-33S.
[23] Zhou YM, Yang YY, Jing YX, Yuan TJ, Sun LH, Tao B, et al. BMP9 reduces bone loss in ovariectomized mice by dual regulation of bone remodeling. J Bone Miner Res 2020;35(5):978–93.
[24] Weischenfeldt J, Porse B. Bone marrow-derived macrophages (BMM): isolation and applications. CSH Protoc 2008;2008. pdb prot5080.
[25] Song C, Yang X, Lei Y, Zhang Z, Smith W, Yan J, et al. Evaluation of efficacy on RANKL induced osteoclast from RAW264.7 cells. J Cell Physiol 2019;234(7):11969–75.
[26] Xie Q, Shen WW, Zhong J, Huang C, Zhang L, Li J. Lipopolysaccharide/adenosine triphosphate induces IL-1beta and IL-18 secretion through the NLRP3 inflammasome in RAW264.7 murine macrophage cells. Int J Mol Med 2014;34(1):341–9.
[27] Trautmann A. Extracellular ATP in the immune system: more than just a "danger signal". Sci Signal 2009;2(56):pe6.
[28] Li X, Ji L, Men X, Chen X, Zhi M, He S, et al. Pyroptosis in bone loss. Apoptosis 2023;28(3–4):293–312.
[29] Huang M, Xu S, Liu L, Zhang M, Guo J, Yuan Y, et al. m6A methylation regulates osteoblastic differentiation and bone remodeling. Front Cell Dev Biol 2021;9:783322.
[30] Bujnicki JM, Feder M, Radlinska M, Blumenthal RM. Structure prediction and phylogenetic analysis of a functionally diverse family of proteins homologous to the MT-A70 subunit of the human mRNA:m(6)A methyltransferase. J Mol Evol 2002;55(4):431–44.
[31] Wang P, Doxtader KA, Nam Y. Structural basis for cooperative function of Mettl3 and Mettl14 methyltransferases. Mol Cell 2016;63(2):306–17.
[32] He M, Lei H, He X, Liu Y, Wang A, Ren Z, et al. METTL14 regulates osteogenesis of bone marrow mesenchymal stem cells via inducing autophagy through m6A/IGF2BPs/beclin-1 signal Axis. Stem Cells Transl Med 2022;11(9):987–1001.
[33] Yang JG, Sun B, Wang Z, Li X, Gao JH, Qian JJ, et al. Exosome-targeted delivery of METTL14 regulates NFATc1 m6A methylation levels to correct osteoclast-induced bone resorption. Cell Death Dis 2023;14(11):738.
[34] Yuan X, Li T, Shi L, Miao J, Guo Y, Chen Y. Human umbilical cord mesenchymal stem cells deliver exogenous miR-26a-5p via exosomes to inhibit nucleus pulposus cell pyroptosis through METTL14/NLRP3. Mol Med 2021;27(1):91.
[35] Hassan MQ, Tare R, Lee SH, Mandeville M, Weiner B, Montecino M, et al. HOXA10 controls osteoblastogenesis by directly activating bone regulatory and phenotypic genes. Mol Cell Biol 2007;27(9):3337–52.
[36] Rux DR, Wellik DM. Hox genes in the adult skeleton: novel functions beyond embryonic development. Dev Dynam 2017;246(4):310–7.
[37] Cao W, Huang H, Xia T, Liu C, Muhammad S, Sun C. Homeobox a5 promotes white adipose tissue browning through inhibition of the tenascin C/Toll-Like receptor 4/nuclear factor kappa B inflammatory signaling in mice. Front Immunol 2018;9:647.
[38] Mao CY, Wang YG, Zhang X, Zheng XY, Tang TT, Lu EY. Double-edged-sword effect of IL-1beta on the osteogenesis of periodontal ligament stem cells via crosstalk between the NF-kappaB, MAPK and BMP/Smad signaling pathways. Cell Death Dis 2016;7:e2296.
[39] Nakamura I, Jimi E. Regulation of osteoclast differentiation and function by interleukin-1. Vitam Horm 2006;74:357–70.
[40] Ruscitti P, Cipriani P, Carubbi F, Liakouli V, Zazzeroni F, Di Benedetto P, et al. The role of IL-1beta in the bone loss during rheumatic diseases. Mediat Inflamm 2015;2015:782382.
[41] Amarasekara DS, Yun H, Kim S, Lee N, Kim H, Rho J. Regulation of osteoclast differentiation by cytokine networks. Immune Netw 2018;18(1):e8.
[42] Dai SM, Nishioka K, Yudoh K. Interleukin (IL) 18 stimulates osteoclast formation through synovial T cells in rheumatoid arthritis: comparison with IL1 beta and tumour necrosis factor alpha. Ann Rheum Dis 2004;63(11):1379–86.
[43] Horwood NJ, Elliott J, Martin TJ, Gillespie MT. IL-12 alone and in synergy with IL-18 inhibits osteoclast formation in vitro. J Immunol 2001;166(8):4915–21.
[44] Liu S, Du J, Li D, Yang P, Kou Y, Li C, et al. Oxidative stress induced pyroptosis leads to osteogenic dysfunction of MG63 cells. J Mol Histol 2020;51(3):221–32.
[45] Chen D, Jiang X, Zou H. hASCs-derived exosomal miR-155-5p targeting TGFbetaR2 promotes autophagy and reduces pyroptosis to alleviate intervertebral disc degeneration. J Orthop Translat 2023;39:163–76.
[46] Chen Y, Liu Y, Jiang K, Wen Z, Cao X, Wu S. Linear ubiquitination of LKB1 activates AMPK pathway to inhibit NLRP3 inflammasome response and reduce chondrocyte pyroptosis in osteoarthritis. J Orthop Translat 2023;39:1–11.